


Cite this: *Dalton Trans.*, 2017, **46**, 5048Ligands and complexes based on piperidine and their exploitation of the ring opening polymerisation of *rac*-lactide†Paul McKeown,<sup>a</sup> James Brown-Humes,<sup>b</sup> Matthew G. Davidson,<sup>a,b</sup> Mary F. Mahon,<sup>b</sup> Timothy J. Woodman<sup>c</sup> and Matthew D. Jones \*<sup>b</sup>

A range of ligands based upon 2-(aminomethyl)piperidine have been successfully complexed to Mg(II), Zn(II) and group IV metal centres. These complexes have been characterised both in solution and solid state with different coordination geometries realised dependant on the nature of the ligand. For the Mg(II) and Zn(II) complexes, M(**1–2**)<sub>2</sub>, were isolated and analysed by DOSY NMR spectroscopy. These ligands also furnished diastereomeric group IV complexes, M(**1–2**)<sub>2</sub>(O<sup>i</sup>Pr)<sub>2</sub>. Group IV salalen and salan complexes, M(**4–5**)(OR)<sub>2</sub> were also found to be diastereomeric in nature, with either  $\beta$ -*cis* or  $\alpha$ -*cis* geometries respectively. The tridentate ligand, **6H**<sub>2</sub>, yielded five coordinate complexes with both Ti(IV) and Zr(IV). All complexes were screened for the ring opening polymerisation of *rac*-lactide under both solvent and melt conditions. For the Mg(II) and Zn(II) complexes, good activity was observed with Zn(**1–2**)<sub>2</sub> demonstrating immortal polymerisation characteristics.

Received 1st March 2017,  
Accepted 22nd March 2017

DOI: 10.1039/c7dt00751e

rsc.li/dalton

## Introduction

There are approximately 300 Mt's of plastics produced annually, of which only 1% are from renewable resources.<sup>1</sup> As well as being bio-based, such renewable materials need to have comparable material properties to conventional plastics to fulfill the same range of applications. Poly(lactic acid) (PLA) has received much interest due to its renewable credentials as well as promising mechanical and biodegradation properties.<sup>2–7</sup> The challenges for PLA are related to the ability to control polymer tacticity, a property which greatly impacts the thermal characteristics of the final material.<sup>8</sup> To achieve this, a wide range of complexes for the ring opening polymerisation (ROP) of lactide (LA) have been detailed in the literature. Success has been achieved with Al(III) complexes, with exquisite stereocontrol often being reported.<sup>9–22</sup> However, a common drawback to Al(III) complexes is low activity, with several days being required to achieve high conversions in

extreme cases.<sup>12,19,20</sup> Although this is not always the case, for example we have shown that Al-salan complexes based on the piperidine back bone can show excellent rates.<sup>15</sup> The use of Ga(III) and In(III) complexes has been shown to increase activity relative to Al(III), but the level of stereocontrol is often much reduced.<sup>23–32</sup> Group I metals have shown to be highly active for the ROP and in some instances, Na(I) and K(I) complexes have demonstrated strong isotactic tendencies.<sup>33–38</sup> Lanthanide based complexes have also received much attention, demonstrating high activities with both heterotactic and isotactic PLA being reported.<sup>39–48</sup>

Relevant to this study is the application of group II, Zn(II) and group IV metal complexes for the ROP of *rac*-LA. Mg(II) and Zn(II) based complexes have been widely reported and represent popular metal choices due to their high abundance and biocompatibility. Such complexes often demonstrate high activity and selectivity. The application of  $\beta$ -diketiminate (BDI) ligands with Mg(II)/Zn(II) typically affords highly active alkoxide bridged species. Coates *et al.* have demonstrated a [(BDI)Zn(O<sup>i</sup>Pr)]<sub>2</sub> complex which facilitates rapid polymerisation at ambient temperatures as well as furnishing highly heterotactic PLA ( $P_r = 0.94$ , 0 °C).<sup>49</sup> A similar result is achievable with (BDI)Mg(O<sup>t</sup>Bu) with the crucial factor being the choice of solvent; Chisholm *et al.* have demonstrated high heterotactic preference ( $P_r = 0.90$ ) for this system but only for polymerisations carried out in THF.<sup>50</sup> Ma *et al.* have reported a series of chiral amino-monophenol ligands with both Mg(II) and Zn(II).<sup>51–54</sup> Due to pro-chirality of a coordinating nitrogen,

<sup>a</sup> Doctoral Training Centre in Sustainable Chemical Technologies, University of Bath, Bath BA2 7AY, UK<sup>b</sup> Department of Chemistry, University of Bath, Claverton Down, Bath BA2 7AY, UK. E-mail: mj205@bath.ac.uk; Fax: +44 (0)1225 386231; Tel: +44 (0)1225 384908<sup>c</sup> Department of Pharmacy and Pharmacology, University of Bath, Claverton Down, Bath BA2 7AY, UK† Electronic supplementary information (ESI) available: Full analysis of <sup>1</sup>H and <sup>13</sup>C{<sup>1</sup>H} NMR spectra and data are provided as well as examples of polymer characterisation. CCDC 1534471–1534479. For ESI and crystallographic data in CIF or other electronic format see DOI: 10.1039/c7dt00751e

diastereomers are generally observed for these complexes. For the Mg(II) family of complexes, both heterotactic ( $P_r = 0.78$ ) and isotactic ( $P_m = 0.67$ ) PLA are achievable in toluene within an hour.<sup>51,53</sup> For the corresponding Zn(II) complexes, an increased isotactic bias ( $P_m = 0.84$ ,  $T_m = 166$  °C) was realised with bulkier ligand substituents.<sup>52,54</sup> Abbina and Du have prepared a series of chiral amido-oxazolinane Zn(II) complexes.<sup>55</sup> These structures contain a three coordinate metal centre and achieve high isotacticity ( $P_m = 0.91$ ,  $T_m = 212$  °C) at room temperature. Redshaw *et al.* have trialled a Mg(II) calixarene complex for the ROP of *rac*-LA.<sup>56</sup> High conversion was achieved in minutes and both heterotactic PLA (THF,  $P_r = 0.85$ ) and isotactic PLA (toluene,  $P_m = 0.70$ ) were realised. Almost perfectly heterotactic PLA has been prepared by Cui,<sup>57</sup> using Mg(II) phosphinimino-amine complexes. High conversion and selectivity was observed at room temperature (THF,  $P_r = 0.93$ ) and this control could be enhanced at 0 °C ( $P_r = 0.98$ ).

A series of group IV imino monophenolate complexes have been prepared by Davidson.<sup>58</sup> The Zr(IV) complexes demonstrated a heterotactic bias under both solution and melt conditions ( $P_r < 0.78$ ) and the system was found to be robust, being resistant to the addition of water. Our work has also focussed on group IV salalen structures.<sup>59</sup> For this family of complexes, optimal results were achieved with Hf(IV) which furnished isotactic PLA ( $P_m < 0.75$ ). Related salan group IV structures were found to demonstrate higher activity and maintained an isotactic bias ( $P_m < 0.75$ ).<sup>60</sup> Use of chiral bipyridine salan complexes increased the degree of stereocontrol and activity ( $P_m < 0.86$ ,  $T_m = 176$  °C), with successful polymerisations being carried out in both solution and solvent free ROP.<sup>21,61</sup> Recently, we have reported a range of complexes based upon 2-(aminomethyl)piperidine (2-AMP) frameworks.<sup>15,22</sup> Imino monophenolate Al(III) complexes were shown to be active for the ROP of *rac*-LA with selectivity and polymerisation rate being greatly influenced by the *ortho* aryl substituents.<sup>22</sup> The related salalen Al(III) complexes had much reduced activity with marginal stereocontrol.<sup>22</sup> Remarkably, the corresponding Al(III) salan complexes demonstrated a dramatic increase in activity and selectivity ( $P_m = 0.83$ ,  $T_m = 177$  °C).<sup>15</sup>

In this study, a range of ligand types (based on 2-AMP) are prepared and complexed to a variety of metal centres. The initial monophenol ligand set is readily converted to a salalen ligand which is reducible to yield a salan. For the monophenol ligands, Mg(II) and Zn(II) complexes are targeted. The bisphenol systems are amenable to coordination to group IV metal centres. The resultant complexes were then tested for their activity in the ROP of *rac*-LA.

## Results and discussion

### Ligand synthesis

The procedure for ligand synthesis (except 2H) has been previously reported (Fig. 1 and 2).<sup>15,22</sup> For the monophenol

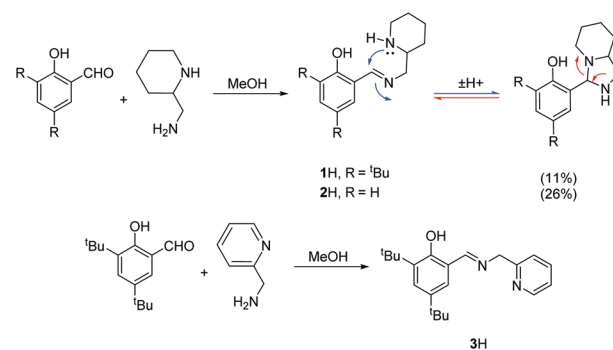


Fig. 1 Synthesis and tautomerism of monophenolate ligands, 1–2H and synthesis of 3H.

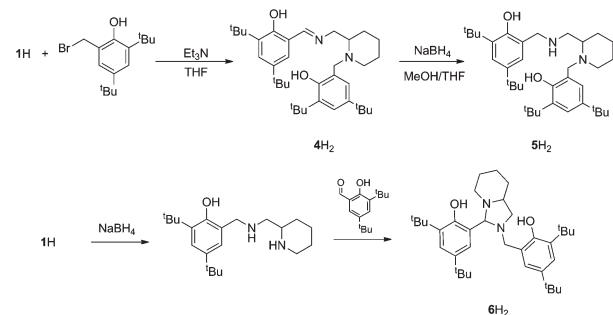


Fig. 2 Synthesis of bisphenol ligands, 4–6H<sub>2</sub>.

ligands, 1H and 2H, a ring-chain tautomer is present in solution leading to a further bicyclic product (Fig. 1).

For the <sup>t</sup>Bu substituted aryl ring (1H), 89% of the product is observed to be the desired imino form and for the unsubstituted aryl ring (2H), 74% of the product is represented by the imino form (CDCl<sub>3</sub>, 298 K). For comparison, a pyridine based ligand, 3H, was prepared according to literature methods.<sup>62</sup> From 1H, both salalen and salan ligands were also realised (Fig. 2). A small amount (<10%) of bicyclic bisphenol, 6H, is typically isolated with the salalen, 4H<sub>2</sub>, and this structure is resistant to reduction and is also present in the salan, 5H<sub>2</sub>. To determine the activity of resultant complex impurities, a route was devised to produce 6H<sub>2</sub> in high yield and purity (Fig. 2).

### Monophenolate complexes

Ligands, 1–2H were complexed to both Mg(II) and Zn(II) (Fig. 3). The pyridine based ligand, 3H, has previously been complexed with Zn(II) and therefore was only complexed to Mg(II).<sup>63,64</sup> Despite a 1 : 1 ligand-to-metal stoichiometry, only the homoleptic complexes, M(1–3)<sub>2</sub> were isolable from reaction with the metal alkyl species. X-ray crystallographic analysis revealed a *pseudo* octahedral complex for M(1)<sub>2</sub> {M = Mg(II) or Zn(II)} (Fig. 4).

The three *trans* groups show deviation between the anticipated 180° bond angle with the more rigid *trans* imino groups being closer to ideality {O(1/2)–Mg–N<sub>p</sub>(2/4) = 158.95(7)°/163.2(2)°, N(1)–Zn–N(3) = 178.62(18)°, O(1)–Zn–N<sub>p</sub>(2) = 165.48(16)°,



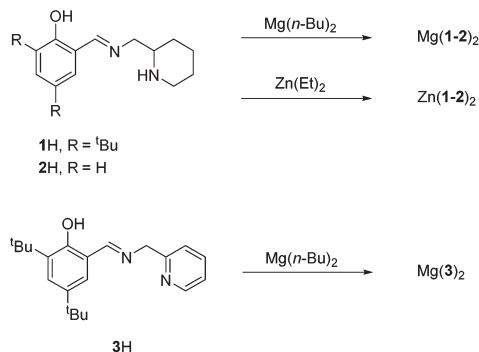


Fig. 3 Synthesis of Mg/Zn(II) monophenolate complexes.

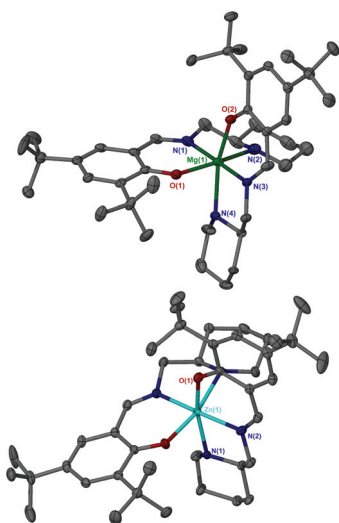


Fig. 4 Solid-state structure of Mg(1)<sub>2</sub> (Top) and Zn(1)<sub>2</sub> (Bottom). Ellipsoids are shown at the 30% probability level and all hydrogen atoms have been removed for clarity. Selected bond length (Å) and angles (°): Mg–O(1) = 1.9963(16), Mg–O(2) = 1.9751(15), Mg–N(1) = 2.1359(18), Mg–N<sub>p</sub>(2) = 2.326(2), Mg–N(3) = 2.105(9), Mg–N(4) = 2.257(7); O(1)–Mg–N<sub>p</sub>(2) = 158.95(7), N(1)–Mg–N(3) = 178.62. Zn–O(1) = 2.0139(12), Zn–N<sub>p</sub>(1) = 2.256(6), Zn–N(2) = 2.1182(14); O(1)–Zn–N(1) = 165.48(16), N(1)–Zn–N(3) = 171.56(8).

N(1)–Zn–N(3) = 171.56(8)°. Within these geometries, a *mer-mer* arrangement of ligands was observed.

For both Mg(II) and Zn(II) complexes of 1H disorder is present in the solid-structure, being centred around the aminopiperidine chiral centre. These secondary positions clearly show an exchange in groups at the chiral centre with the ring “flipped” to maintain the imino methyl group in the equatorial position (Fig. 5). These two structures are represented in the form of diastereomeric pairs in the form of (*RR/RS*) and (*SS/SR*), for both Mg(1)<sub>2</sub> and Zn(1)<sub>2</sub>. A similar solid-state geometry is anticipated for Mg/Zn(2)<sub>2</sub>.

The presence of diastereomers for Mg/Zn(1/2)<sub>2</sub> is supported by <sup>1</sup>H NMR spectroscopy, which shows multiple species in solution. These species typically occur within narrow chemical shift ranges, suggesting similar environments. DOSY NMR

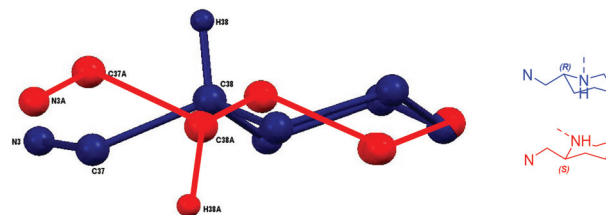
Fig. 5 Disordered positions of piperidine ring in Mg(1)<sub>2</sub>.

Table 1 Diffusion coefficients ( $\times 10^{-10} \text{ m}^2 \text{ s}^{-1}$ ) of Mg(1)<sub>2</sub>, Zn(1)<sub>2</sub>, and 1H (C<sub>6</sub>D<sub>6</sub>, 298 K)

	Mg(1) <sub>2</sub>	Zn(1) <sub>2</sub>	1H
Major	4.78	5.56	6.87
Minor	4.67	5.47	

spectroscopy of both Mg(1)<sub>2</sub> and Zn(1)<sub>2</sub> revealed two distinct sets of diffusion coefficients with a small difference be  $4.67 \times 10^{-10} \text{ m}^2 \text{ s}^{-1}$  and  $4.78 \times 10^{-10} \text{ m}^2 \text{ s}^{-1}$  (C<sub>6</sub>D<sub>6</sub>, 298 K) (Table 1).

Larger values are found for Zn(1)<sub>2</sub>, equal to  $5.47 \times 10^{-10} \text{ m}^2 \text{ s}^{-1}$  and  $5.56 \times 10^{-10} \text{ m}^2 \text{ s}^{-1}$  (C<sub>6</sub>D<sub>6</sub>, 298 K). The close agreement of these values for each complex series is further evidence that the samples are isomeric. For comparison, the diffusion coefficient of the free ligand is also given; uncoordinated 1H diffuses at a faster rate relative to the complexes ( $6.87 \times 10^{-10} \text{ m}^2 \text{ s}^{-1}$  (C<sub>6</sub>D<sub>6</sub>, 298 K)).

For 3H, without any potential point of chirality, the <sup>1</sup>H and <sup>13</sup>C{<sup>1</sup>H} spectra of the resultant Mg(II) complex reveal one species in solution. Hence, an octahedral complex is likely present in solution in an analogous fashion to Mg(1)<sub>2</sub>. Unlike the free ligand, the –CH<sub>2</sub>– groups connected to the pyridine moiety are now split into a pair of diastereotopic doublets, indicating their inequivalence once coordinated.

#### Group IV complexes

Complexation of the imino monophenol, 1H, to group IV metals yielded M(1)<sub>2</sub>(O<sup>i</sup>Pr)<sub>2</sub>, where M = Ti(IV) or Zr(IV) (Fig. 6). Complexes based upon 1H, M(1)<sub>2</sub>(O<sup>i</sup>Pr)<sub>2</sub>, were characterised by X-ray crystallography revealing a *pseudo* octahedral geometry in each case (Fig. 7). The arrangement of ligands around the metal centre conforms to an  $\alpha$ -*cis* conformation with *trans* phenoxy groups {O(3)–Ti–O(4) = 167.12(5)°/O(3)–Zr–O(4) = 163.02(5)°} and *cis* isopropoxide moieties {O(1)–Ti–O(2) = 104.60(6)°/O(1)–Zr–O(2) = 101.64(6)°}. The solid-state structure is a racemate with a  $\Delta$ -SS/ $\Lambda$ -RR configuration. Comparison of the bond lengths and angles for both Ti(1)<sub>2</sub>(O<sup>i</sup>Pr)<sub>2</sub> and Zr(1)<sub>2</sub>(O<sup>i</sup>Pr)<sub>2</sub> show both complexes to be similar and

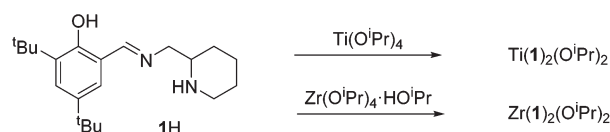
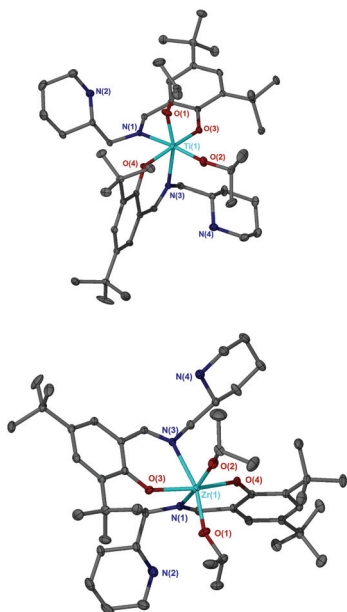


Fig. 6 Synthesis of group IV monophenolate complexes.





**Fig. 7** Solid-state structure of  $\Delta$ -Ti(SS-1) $_2$ (OiPr) $_2$  (Top) and  $\Lambda$ -Zr(RR-1) $_2$ (OiPr) $_2$  (Bottom). Ellipsoids are shown at the 30% probability level and all hydrogen atoms have been removed for clarity. Selected bond length (Å) and angles (°): Ti–O(1) = 1.8037(12), Ti–O(2) = 1.7852(12), Ti–O(3) = 1.9473(10), Ti–O(4) = 1.9316(10), Ti–N(1) = 2.2628(13), Ti–N(3) = 2.2825(12); O(1)–Ti–O(2) = 104.60(6), O(1)–Ti–N(3) = 162.39(5), O(3)–Ti–O(4) = 167.12(5). Zr–O(1) = 1.9245(13), Zr–O(2) = 1.9289(13), Zr–O(3) = 2.0587(11), Zr–O(4) = 2.0596(12), Zr–N(1) = 2.3979(14), Zr–N(3) = 2.3979(14); O(1)–Zr–O(2) = 104.64(6), O(1)–Zr–N(3) = 161.42(6), O(3)–Zr–O(4) = 163.02(5).

compare well to related literature complexes in terms of their metric data.<sup>58</sup>

Analysis of the  $^1\text{H}$  NMR spectra for  $\text{M}(\text{1-2})_2(\text{O}^i\text{Pr})_2$  revealed multiple species in solution (Fig. 8). This is to be expected due to the potential for diastereomeric relationships, with three points of chirality in the structure. It is assumed that the major isomer is that observed for the crystal structure ( $\Delta$ -SS/ $\Lambda$ -RR) and the remaining species are due to the remaining diastereomers (*e.g.*,  $\Delta$ -RS/ $\Lambda$ -SR or  $\Lambda$ -RS/ $\Delta$ -SR). Similar observations and assignments have been previously reported.<sup>58</sup> The  $^{13}\text{C}\{^1\text{H}\}$  NMR spectra provides further evidence for the species to be related diastereomers, having four distinct resonances for the

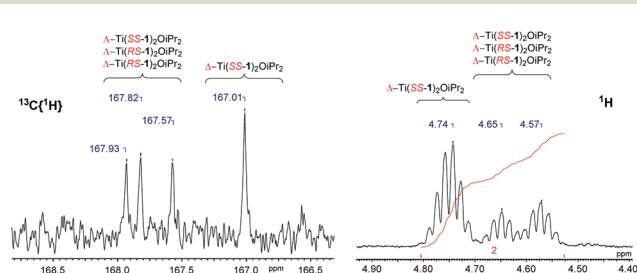


**Fig. 8**  $^{13}\text{C}\{^1\text{H}\}$  NMR spectrum showing imino region and  $^1\text{H}$  NMR spectrum showing methine region of  $\text{Ti}(\text{1})_2(\text{O}^i\text{Pr})_2$ . Diastereomers have only been indicated but are present as enantiomeric pairs.

imino functionality in agreement with the number of inequivalent species (Fig. 8). Further analysis *via* DOSY NMR spectroscopy suggests the species in solution are diffusing at a similar rate [ $\text{CDCl}_3$ , 298 K,  $\text{Ti}(\text{1})_2(\text{O}^i\text{Pr})_2$ ,  $D = 5.47 \times 10^{-10} \text{ m}^2 \text{ s}^{-1}$ / $\text{Zr}(\text{1})_2(\text{O}^i\text{Pr})_2$ ,  $D = 4.35 \times 10^{-10} \text{ m}^2 \text{ s}^{-1}$ ].

The complexation of 3H to  $\text{Ti}(\text{O}^i\text{Pr})_4$  afforded an unexpected product. Instead of the anticipated bis-ligated species,  $\text{Ti}(\text{3})_2(\text{O}^i\text{Pr})_2$ , the isolated complex is the product of a ligand dimerisation (Fig. 9, and ESI†). The resultant  $\text{Ti}(\text{iv})$  salalen complex is shown to adopt an octahedral geometry in the solid-state with a  $\beta$ -*cis* arrangement of coordinating groups. The new carbon chiral centres are observed to have opposing stereochemical configurations and the titanium centre also possesses chirality ( $\Lambda$ -RS/ $\Delta$ -SR).

Analysis of  $\text{Ti}(\text{3}^*)(\text{O}^i\text{Pr})_2$  by  $^1\text{H}/^{13}\text{C}\{^1\text{H}\}$  NMR spectroscopy reveals an increased number of  $-\text{CH}_2-$  and  $-\text{CH}-$  resonances due to the ligand dimerisation. A NH resonance is also identifiable in the  $^1\text{H}$  spectra. Resonances related to inequivalent isopropoxide groups are also observed suggesting the solid-state structure is maintained in solution. There are also several species observed for this complex.

From the complex filtrate, a second precipitate was isolated. Subsequent analysis of which revealed a different NMR spectrum which was also consistent with the structure of  $\text{Ti}(\text{3}^*)(\text{O}^i\text{Pr})_2$  with increased purity. It is suggested that the second product is a diastereomer, for which the chirality at the two carbon centres is the same ( $\text{RR}/\text{SS}$ ).

The complexation of 3H with  $\text{Zr}(\text{iv})$  afforded the expected bis-ligated product as shown by NMR spectroscopy. The number of resonances indicates an equivalence of both ligands and isopropoxide groups suggesting an  $\alpha$ -*cis* conformation. There is a broadness associated with the isopropoxide and a  $-\text{CH}_2-$  benzylic resonances which is resolved on cooling ( $\text{CDCl}_3$ , 273 K).

The salalen,  $4\text{H}_2$ , was also successfully coordinated to  $\text{Ti}(\text{iv})$  and  $\text{Zr}(\text{iv})$ . For the  $\text{Zr}(\text{iv})$  complexation, best results were

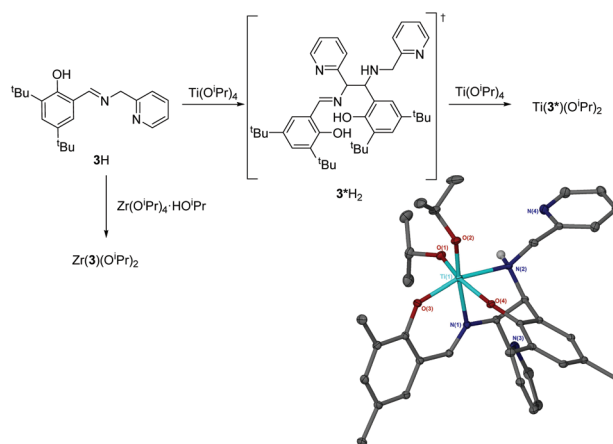


**Fig. 9** Group IV complexes of 3H. Solid-state structure of  $\text{Ti}(\text{3}^*)(\text{O}^i\text{Pr})_2$ . Ellipsoids are shown at the 30% probability level and all hydrogen atoms have been removed for clarity.



achieved by employing  $\text{Zr}(\text{O}^t\text{Bu})_4$ , which furnished a complex amenable to recrystallisation. The use of  $\text{Zr}(\text{O}^i\text{Pr})_4 \cdot (\text{HO}^i\text{Pr})$  afforded the desired product, as suggested by  $^1\text{H}$  NMR analysis, but the complex was not successfully purified. Solid-state analysis of both metal complexes revealed a *pseudo* octahedral structure with a  $\beta$ -*cis* geometry (Fig. 10 and 11). The alkoxide groups have a *cis* relationship  $\{\text{O}(1)\text{--Ti--O}(2) = 92.57(5)^\circ/\text{O}(1)\text{--Zr--O}(2) = 96.75(4)^\circ\}$  and the phenoxy groups of both complexes are also mutually *cis* for  $\{\text{O}(3)\text{--Ti--O}(4) = 90.30(6)^\circ/\text{O}(3)\text{--Zr--O}(4) = 91.45(5)^\circ\}$ . The imino bond-to-metal is observed to be shorter relative to the amino bond {for  $\text{Zr}(\text{4})(\text{O}^t\text{Bu})_2$ ,  $\text{Zr--N}(1) = 2.3417(16) \text{ \AA}$  vs.  $\text{Zr--N}(2) = 2.3417(16) \text{ \AA}$ }. The stereochemical configuration of both complexes is observed to be  $\Lambda$ -*RS*/ $\Delta$ -*SR*. The ligand wrapping and bond lengths/angles are consistent with group IV complexes reported in the literature.<sup>65–67</sup>

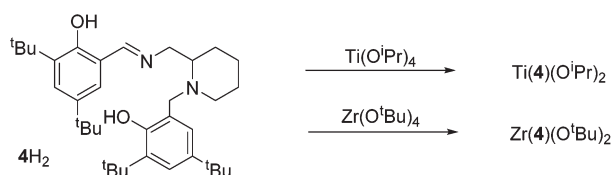


Fig. 10 Synthesis of group IV salalen complexes.

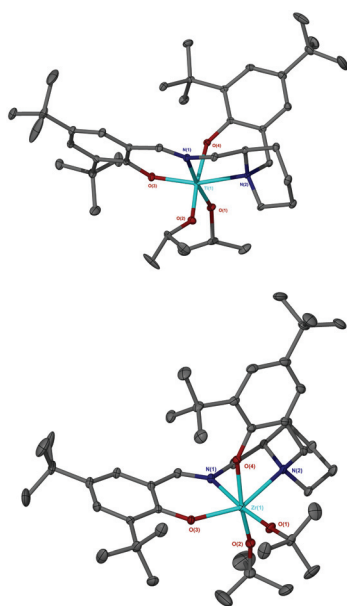


Fig. 11 Solid-state structure of  $\Lambda$ -*Ti*(*RS*-4)(*O*<sup>*i*</sup>*Pr*)<sub>2</sub> (Top) and  $\Delta$ -*Zr*(*SR*-4)(*O*<sup>*t*</sup>*Bu*)<sub>2</sub> (Bottom). Ellipsoids are shown at the 30% probability level and all hydrogen atoms have been removed for clarity. Selected bond length (Å) and angles (°):  $\text{Ti--O}(1) = 1.8351(11)$ ,  $\text{Ti--O}(2) = 1.8537(12)$ ,  $\text{Ti--O}(3) = 1.8890(12)$ ,  $\text{Ti--O}(4) = 1.9257(11)$ ,  $\text{Ti--N}(1) = 2.2038(13)$ ,  $\text{Ti--N}(2) = 2.3101(13)$ ;  $\text{O}(1)\text{--Ti--O}(2) = 92.57(5)$ ,  $\text{O}(1)\text{--Ti--N}(1) = 169.83(5)$ ,  $\text{O}(3)\text{--Ti--O}(4) = 91.79(5)$ .  $\text{Zr--O}(1) = 1.9398(14)$ ,  $\text{Zr--O}(2) = 1.9535(14)$ ,  $\text{Zr--O}(3) = 2.0209(12)$ ,  $\text{Zr--O}(4) = 2.0731(13)$ ,  $\text{Zr--N}(1) = 2.3417(16)$ ,  $\text{Zr--N}(2) = 2.4371(15)$ ;  $\text{O}(1)\text{--Zr--O}(2) = 96.75(4)$ ,  $\text{O}(1)\text{--Zr--N}(1) = 174.48(6)$ ,  $\text{O}(3)\text{--Zr--O}(4) = 163.02(5)$ .

Analysis *via*  $^1\text{H}$  NMR spectroscopy reveals two species in solution at a ratio of approximately 5 : 1 for both salalen  $\text{Ti}(\text{iv})$  and  $\text{Zr}(\text{iv})$  complexes (Fig. 12). It is proposed that the minor series of resonances is due to the presence of diastereomers in solution. Application of achiral salalens typically lead to the formation of single diastereomers in solution despite the chirality at both metal and nitrogen centres.<sup>65–67</sup> It is therefore tentatively suggested that the extra resonances are due to  $\Lambda$ -*SS*/ $\Delta$ -*RR* species, with the metal and nitrogen chirality remaining unchanged.

Coordination of the related salan,  $5\text{H}_2$ , with group IV metals was also realised (Fig. 13). For  $\text{Ti}(5)(\text{O}^i\text{Pr})_2$  due to the reduction of the imino functionality, an  $\alpha$ -*cis* geometry is adopted having a *trans* relationship between phenoxy groups  $\{\text{O}(3)\text{--Ti--O}(4) = 161.33(5)^\circ\}$ . The two isopropoxide groups are observed to be mutually *cis*  $\{\text{O}(1)\text{--Ti--O}(2) = 105.58(6)^\circ\}$  in the structure of  $\text{Ti}(5)(\text{O}^i\text{Pr})_2$ . The nitrogen centre within the piperidine ring has a lengthened bond relative to that of the secondary amine  $\{\text{Ti--N}_\text{p}(1) = 2.3876(13) \text{ \AA}/\text{Ti--N}(2) = 2.2797(13) \text{ \AA}\}$ . The stereochemical configuration of the ligand is observed to be *SRS*/*RSR* relating to the nitrogen, carbon and nitrogen centres respectively. The metric data for  $\text{Ti}(5)(\text{O}^i\text{Pr})$  is consistent with that of literature  $\text{Ti}(\text{iv})$  salan complexes.<sup>60,68–70</sup> The related  $\text{Zr}(\text{iv})$  complex,  $\text{Zr}(5)(\text{O}^t\text{Bu})_2$  is assumed to adopt a similar geometry to the  $\text{Ti}(\text{iv})$  analogue. Investigation of the solution state structure of  $\text{Ti}(5)(\text{O}^i\text{Pr})_2$  by  $^1\text{H}$  NMR spectroscopy revealed a minor series which corresponds to ~10%. Nevertheless, the resonances of the major product correlate to the solid-state structure of  $\text{Ti}(5)(\text{O}^i\text{Pr})_2$ . While likely diastereotopic in nature, the exact assignment of the extra resonances is increasingly

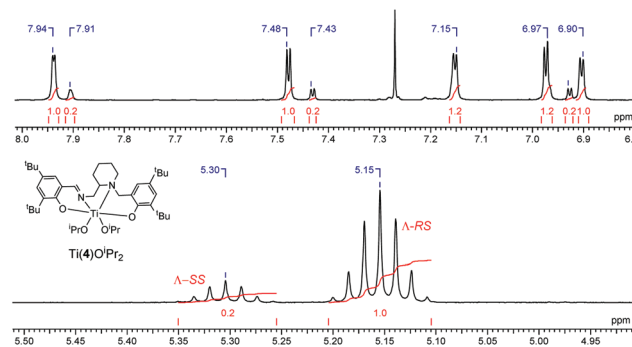


Fig. 12  $^1\text{H}$  NMR ( $\text{CDCl}_3$ , 298 K) spectra of  $\text{Ti}(4)(\text{O}^i\text{Pr})_2$  showing imino-aromatic region and methine region with  $\Lambda$ -*RS* and  $\Lambda$ -*SS* assignment. Diastereomers have only been indicated but are present as enantiomeric pairs.

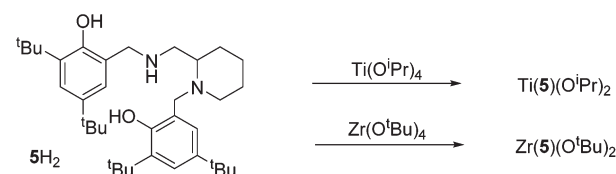


Fig. 13 Synthesis of group IV salan complexes.



complex due to four points of chirality for  $\text{Ti}(\text{5})(\text{O}^i\text{Pr})_2$ . Previous reports concerning the coordination of chiral ligands to  $\text{Ti}(\text{IV})$  have demonstrated a change in chirality at the metal centre is common for these systems.<sup>68,70,71</sup> A switch to  $\Delta$  chirality at the metal could be the origin of the diastereomers for this system, with the  $\Delta$  chirality being preferred during synthesis or recrystallisation (Fig. 14). In contrast, the  $^1\text{H}$  NMR spectrum for  $\text{Zr}(\text{5})(\text{O}^i\text{Bu})_2$  revealed the presence of a pure complex in solution.

The bicyclic ligand,  $\text{6H}_2$ , was also coordinated to group IV metals (Fig. 15). Complexation with  $\text{Zr}(\text{O}^i\text{Bu})_4$  afforded the crystalline product,  $\text{Zr}(\text{6})(\text{O}^i\text{Bu})_2$ . The complex geometry is observed to be trigonal bipyramidal with a *tert*-butoxide and amine group occupying the *pseudo* axial positions  $\{\text{N}(1)-\text{Zr}-\text{O}(1) = 168.83(7)^\circ\}$  (Fig. 16). Use of a bulkier  $\text{Zr}(\text{IV})$  source as well as sterically demanding aryl groups furnishes exclusively the alkoxide complex; we have previously reported a related series of  $\text{Zr}(\text{IV})$  complexes that demonstrated a strong tendency in forming the bis-ligated species,  $\text{Zr}(\text{L})_2$ .<sup>22</sup>

The metric data is similar to that of a related  $\text{Ti}(\text{IV})$  complex published previously, albeit with a reduced ideality towards the trigonal bipyramidal geometry ( $\tau = 0.78$ ).<sup>22</sup> Analysis of both  $\text{Zr}(\text{IV})$  and  $\text{Ti}(\text{IV})$  complexes of  $\text{6H}_2$  *via* NMR spectroscopy demonstrates the maintaining of the solid-state structure in solution and the presence of a single species.

### Polymerisation studies

Polymerisations were carried out with *rac*-LA which was singly recrystallised before use. Polymerisations with  $\text{Mg}(\text{1-3})_2$  and

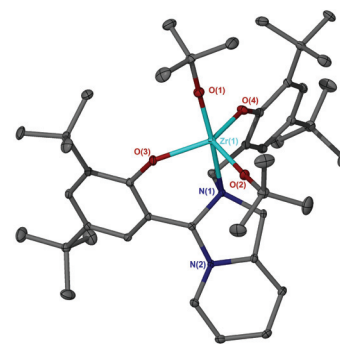


**Fig. 16** Solid-state structure of  $\text{Zr}(\text{6})(\text{O}^i\text{Bu})_2$ . Ellipsoids are shown at the 30% probability level and all hydrogen atoms have been removed for clarity. Selected bond length (Å) and angles ( $^\circ$ ):  $\text{Zr}-\text{O}(1) = 1.9229(18)$ ,  $\text{Zr}-\text{O}(2) = 1.9300(17)$ ,  $\text{Zr}-\text{O}(3) = 2.0181(18)$ ,  $\text{Zr}-\text{O}(4) = 1.9890(18)$ ,  $\text{Zr}-\text{N}(1) = 2.420(2)$ ;  $\text{O}(1)-\text{Zr}-\text{O}(2) = 104.28(8)$ ,  $\text{O}(1)-\text{Zr}-\text{N}(1) = 168.83(7)$ ,  $\text{O}(3)-\text{Zr}-\text{O}(4) = 122.23(8)$ .

$\text{Zn}(\text{1-2})_2$  were performed in solution (toluene) at  $80^\circ\text{C}$ . In the first instance, an equivalence of benzyl alcohol was added to aid initiation (Table 2). For the majority of complexes, high conversion was achievable within one hour, with the  $\text{Zn}(\text{II})$  complexes generally displaying greater activity. In exception to this,  $\text{Mg}(\text{2})_2$  was shown to be less active in this time frame. The PLA produced by these complexes was essentially atactic.

**Table 2**  $\text{Mg}(\text{II})$  and  $\text{Zn}(\text{II})$  complexes for polymerisation of *rac*-LA

Complex	Time/h	Conv. <sup>g</sup> , %	$P_r$ <sup>h</sup>	$M_{n,\text{theo}}$ <sup>i</sup>	$M_n$ <sup>j</sup>	$D^j$
$\text{Mg}(\text{1})_2$ <sup>a</sup>	1	72	0.51	10 500	8300	1.10
$\text{Mg}(\text{2})_2$ <sup>a</sup>	1	40	0.47	6450	2100	1.10
$\text{Mg}(\text{3})_2$ <sup>a</sup>	1	81	0.53	11 800	10 000	1.10
$\text{Zn}(\text{1})_2$ <sup>a</sup>	0.08	90	0.57	13 050	10 550	1.05
$\text{Zn}(\text{1})_2$ <sup>b</sup>	0.5	95	0.57	13 800	12 200	1.10
$\text{Zn}(\text{2})_2$ <sup>a</sup>	0.25	74	0.56	9300	6650	1.08
$\text{Zn}(\text{2})_2$ <sup>b</sup>	0.5	58	0.59	8300	8050	1.05
$\text{Mg}(\text{1})_2$ <sup>c</sup>	1	17	0.53	2600	28 800	1.14
$\text{Mg}(\text{3})_2$ <sup>c</sup>	1	25	0.52	3700	48 450	1.19
$\text{Zn}(\text{1})_2$ <sup>c</sup>	0.5	41	0.58	6000	82 300	1.28
$\text{Zn}(\text{2})_2$ <sup>c</sup>	0.5	9	0.59	1400	28 300	1.07
$\text{Mg}(\text{1})_2$ <sup>d</sup>	0.5	61	0.61	26 450	23 250	1.81
$\text{Mg}(\text{1})_2$ <sup>e</sup>	0.5	74	0.60	32 050	17 400	1.49
$\text{Mg}(\text{2})_2$ <sup>e</sup>	1.5	67	0.57	29 050	5550	1.57
$\text{Mg}(\text{3})_2$ <sup>d</sup>	0.07	53	0.66	23 000	28 100	1.43
$\text{Mg}(\text{3})_2$ <sup>e</sup>	0.07	63	0.66	27 300	22 000	1.41
$\text{Zn}(\text{1})_2$ <sup>d</sup>	0.15	49	0.59	21 250	42 300	1.37
$\text{Zn}(\text{1})_2$ <sup>e</sup>	0.1	69	0.57	29 900	32 250	1.18
$\text{Zn}(\text{1})_2$ <sup>f</sup>	0.3	69	0.57	29 900	24 750	1.12
$\text{Zn}(\text{2})_2$ <sup>e</sup>	1.5	84	0.51	36 700	7650	1.51

Conditions: <sup>a</sup>  $[\text{LA}]:[\text{I}]:[\text{BnOH}] = 100:1:1$ ,  $80^\circ\text{C}$ , toluene. <sup>b</sup>  $[\text{LA}]:[\text{I}] = 1000:1:10$ ,  $80^\circ\text{C}$ , toluene. <sup>c</sup>  $[\text{LA}]:[\text{I}]:[\text{BnOH}] = 100:1$ ,  $80^\circ\text{C}$ , toluene. <sup>d</sup>  $[\text{LA}]:[\text{I}] = 300:1$ ,  $130^\circ\text{C}$ . <sup>e</sup>  $[\text{LA}]:[\text{I}]:[\text{BnOH}] = 300:1:1$ ,  $130^\circ\text{C}$ . <sup>f</sup>  $[\text{LA}]:[\text{I}]:[\text{BnOH}] = 3000:1:10$ ,  $130^\circ\text{C}$ . <sup>g</sup> Determined *via*  $^1\text{H}$  NMR spectroscopy. <sup>h</sup>  $P_r$  is the probability of heterotactic enchainment, determined *via* homonuclear decoupled  $^1\text{H}$  NMR spectroscopy. <sup>i</sup> Theoretical molecular weight calculated from conversion  $\{[\text{LA}]/[\text{BnOH}] \times (\text{conv.} \times 144.13) + 108.14\}$  (rounded to the nearest 50). <sup>j</sup> Determined from GPC (in THF) referenced against polystyrene standards with a correction factor of 0.58 applied.

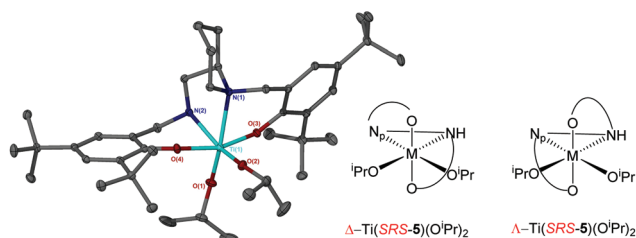


**Fig. 14** Solid-state structure of  $\Delta\text{-Ti}(\text{SRS-5})(\text{O}^i\text{Pr})_2$  and potential diastereomeric configuration. Ellipsoids are shown at the 30% probability level and all hydrogen atoms have been removed for clarity. Selected bond length (Å) and angles ( $^\circ$ ):  $\text{Ti}-\text{O}(1) = 1.8079(12)$ ,  $\text{Ti}-\text{O}(2) = 1.7906(12)$ ,  $\text{Ti}-\text{O}(3) = 1.9138(11)$ ,  $\text{Ti}-\text{O}(4) = 1.9121(11)$ ,  $\text{Ti}-\text{N}(1) = 2.3876(13)$ ,  $\text{Ti}-\text{N}(2) = 2.2797(13)$ ;  $\text{O}(1)-\text{Ti}-\text{O}(2) = 105.58(6)$ ,  $\text{O}(1)-\text{Ti}-\text{N}(1) = 163.11(5)$ ,  $\text{O}(3)-\text{Ti}-\text{O}(4) = 161.33(5)$ .

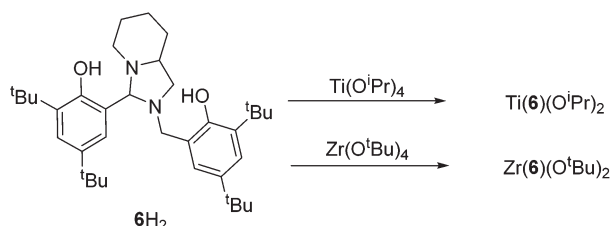


**Fig. 15** Synthesis of group IV salan complexes.

There was very little difference between the activity and stereo-control exerted by  $\text{Mg(1)}_2$  and  $\text{Mg(3)}_2$ .

For this series of complexes, it was found that the addition of excess alcohol, during the polymerisation quenching process, facilitated depolymerisation reactions. This is illustrated by GPC traces of such polymer before and after MeOH wash which show a broadening of the polymer chain distribution {for  $\text{Mg(1)}_2$ , see ESI†}. As a consequence of this, further polymerisations were not quenched. Such observations have previously been noted in the literature.<sup>72,73</sup> This depolymerisation was found to be more pronounced for  $\text{Mg(1)}_2$  which lead to the rapid formation of oligomers and lactates, whereas for  $\text{Zn(1)}_2$  treatment with methanol resulted in a broadening of the GPC trace and a tail towards low molecular weight. It is also noted that  $\text{Mg(3)}_2$  initially afforded a pale yellow polymer which became red on prolonged exposure to air. This has previously been observed and attributed to a ligand oxidation process.<sup>63</sup> The  $\text{Zn(II)}$  complexes were also active with under immortal polymerisation conditions ( $[\text{LA}]:[\text{Zn}]:[\text{BnOH}] = 1000:1:10$ ), achieving reasonable conversion with molecular weight being dependent on the  $[\text{LA}]:[\text{BnOH}]$  ratio. An NMR scale polymerisation was carried out for  $\text{Zn(1)}_2$  ( $\text{CDCl}_3$ , 298 K,  $[\text{LA}]:[\text{Zn}]:[\text{BnOH}] = 20:1:1$ ). The initial combination of complexes and alcohol demonstrated the  $\text{Zn(II)}$  complex to be inert towards alcoholysis. On addition of *rac*-LA, polymer was observed to be produced without any change in the complex resonances suggesting the operation of an activated monomer mechanism (see ESI†). Further to this, DOSY analysis of the system suggested there was no major interaction between polymer and  $\text{Zn(II)}$  centre. Kinetic analysis of the polymerisation with  $\text{Zn(2)}_2$  (toluene, 353 K,  $[\text{LA}]:[\text{Zn}]:[\text{BnOH}] = 100:1:1$ ) yielded a linear plot of  $\ln([\text{LA}]_0/[\text{LA}]_t)$  against time ( $k_{\text{app}} = 5.21 \pm 0.51 \text{ h}^{-1}$ ) indicating the polymerisation proceeds with a first order dependence on monomer (see ESI†).

The resultant molecular weight of solution polymerisations with BnOH co-initiator demonstrates a reasonable correlation with the predicted value. However, the molecular weight achieved by  $\text{Mg(2)}_2$ , is much lower than anticipated. In each case, the distribution of molecular weights is narrow again implying a controlled polymerisation ( $D \leq 1.10$ ). Further analysis *via* MALDI-ToF mass spectrometry gives comparable values of molecular weight and generally shows the presence of polymer chains with a BnO- and -H end groups (see ESI, Table S1†). For each  $\text{Mg(1/3)}$  complex, there is a minor series due to transesterification side reactions. For  $\text{Mg(3)}_2$  there is also evidence of intramolecular transesterification with low molecular weight cyclic oligomers being observed. For  $\text{Mg(2)}_2$ , only cyclic species are observed.

Analysis of polymer derived from  $\text{Zn(1/2)}_2$  *via* MALDI-ToF mass spectrometry indicates a minimal degree of undesirable transesterification reactions. The literature complex,  $\text{Zn(3)}_2$ , was shown to be active in the absence of co-initiator under solution conditions.<sup>64</sup> Under similar conditions, the activity of the complexes  $\text{Mg(1/3)}_2$  and  $\text{Zn(1-2)}_2$  is observed to be much reduced within the same time frame, with  $\text{Zn(1)}_2$  being the most active. Despite the low conversion, relatively high mole-

cular weights are afforded with the distribution of polymer chain remaining relatively narrow. It is unclear if initiation is due to a ligand phenoxy moiety or monomer impurities (see ESI†).

The complexes are also tested under solvent free conditions (130 °C,  $[\text{LA}]:[\text{I}] = 300:1$  or  $[\text{LA}]:[\text{I}] = 300:1:1$ ). The polymerisations with  $\text{Mg(1)}_2$  was hampered by the insolubility of this complex in the molten LA. As a consequence, the reaction time was lengthened. The molecular weight control afforded by these complexes is poor, with lower than theoretical values being realised, even in the absence of BnOH. However, slight heterotacticity is demonstrated by these  $\text{Mg(II)}$  systems ( $P_r \approx 0.60$ ). A faster reaction, with slightly more of a heterotactic preference, is achieved with  $\text{Mg(3)}_2$ , which was fully soluble in the LA melt. A more controlled polymerisation is achieved by employing  $\text{Zn(1)}_2$ , which is also fully soluble in the LA melt. At this higher temperature, the reaction in the absence of benzyl alcohol achieves higher conversion, indicating the initiation step may have a thermal barrier, perhaps due to insertion of a ligand phenoxy moiety. Under these conditions, a higher molecular weight than predicted is afforded, indicating fewer chains are initiated relative to the amount of metal centres. The addition of BnOH yields PLA with a good agreement between experimental molecular weight and predicted.  $\text{Zn(1)}_2$  can also perform under immortal melt conditions (3000:1:10, 130 °C). While there is a slight increase in polymerisation time, the molecular weight achieved is comparable to the LA to co-initiator ratio, with a relative improvement of polymer chain distribution. The solvent-free polymerisation of  $\text{Mg/Zn(2)}_2$  was slow and poorly controlled. It is tentatively suggested that the less hindered metal centres are susceptible to decomposition under these conditions. The titanium based complexes were tested under melt conditions (130 °C, 300:1), having isopropoxide groups to initiate polymerisation directly (Table 3). The bis-ligated complex,  $\text{Ti(1)}_2(\text{O}^i\text{Pr})_2$ , was found to be a poor complexes for the ROP of *rac*-LA achieving 58% under melt conditions after 24 hours. The observed molecular weight is much lower than anticipated suggesting the formation of oligomers. The salalen complexes,  $\text{Ti(3*/4)}(\text{O}^i\text{Pr})_2$ , were observed to only reach 15–17% conversion after 24 hours under these conditions. In this instance, coordination of LA

**Table 3**  $\text{Ti(IV)}$  complexes for polymerisation of *rac*-LA

Complex	Time/h	Conv. <sup>a</sup> , %	$P_r$ <sup>b</sup>	$M_{n,\text{theo}}$ <sup>c</sup>	$M_n$ <sup>d</sup>	$D^d$
$\text{Ti(1)}_2(\text{O}^i\text{Pr})_2$	24	58	0.49	12 550	2850	1.36
$\text{Ti(3*)}(\text{O}^i\text{Pr})_2$	24	15	—	—	—	—
$\text{Ti(4)}(\text{O}^i\text{Pr})_2$	24	17	—	—	—	—
$\text{Ti(5)}(\text{O}^i\text{Pr})_2$	3	75	0.52	16 250	13 900	1.04
$\text{Ti(6)}(\text{O}^i\text{Pr})_2$	18	72	0.51	15 550	10 350	1.31

Conditions:  $[\text{LA}]:[\text{I}] = 300:1$ , 130 °C, solvent free. <sup>a</sup> Determined *via*  $^1\text{H}$  NMR spectroscopy. <sup>b</sup>  $P_r$  is the probability of heterotactic enchainment, determined *via* homonuclear decoupled  $^1\text{H}$  NMR spectroscopy. <sup>c</sup> Theoretical molecular weight calculated from conversion  $\{300 \times (\text{conv.} \times 144.13) + M_n(\text{end group})\}/2$  (rounded to the nearest 50). <sup>d</sup> Determined from GPC (in THF) referenced against polystyrene standards with a correction factor of 0.58 applied.



may be restricted due to high metal coordination and bulky aryl substituents. The titanium salan complex,  $\text{Ti}(5)(\text{O}^i\text{Pr})_2$  is more active reaching high conversion within 3 hours. The  $\text{Ti}(\text{IV})$  salan complex affords a narrow distribution of polymer chains with a molecular weight consistent with two chain per metal centre. Geometrically, the structures are different with the salalen adopting a *fac-mer* geometry and the salan, a *fac-fac* arrangement. This increased activity on going from salalen to salan also correlates with the observations made for the respective aluminium complexes.<sup>15,22</sup>

The bicyclic complex  $\text{Ti}(6)(\text{O}^i\text{Pr})_2$  achieved reasonable conversion within 18 hours, however, molecular weight control was poor ( $\bar{D} = 1.31$ ). The activity of  $\text{Ti}(6)(\text{O}^i\text{Pr})_2$  is much reduced compared to a previously reported bicyclic analogue.<sup>22</sup> In no instance is stereocontrol exerted by this series of complexes which is analogous to the majority of  $\text{Ti}(\text{IV})$  complexes in the literature.<sup>58,66,74–77</sup>

The bis-ligated species,  $\text{Zr}(1)_2(\text{O}^i\text{Pr})_2$  was more active than the related  $\text{Ti}(\text{IV})$  complex,  $\text{Ti}(1)_2(\text{O}^i\text{Pr})_2$ . In solution (toluene, 80 °C), reasonable conversion was achieved after 2 hours and under solvent free conditions, less than 1 hour was required. However, similar to the  $\text{Ti}(\text{IV})$  complex, only lower molecular weight was achievable. In comparison,  $\text{Zr}(3)_2(\text{O}^i\text{Pr})_2$  achieves a higher molecular weight with improved control albeit with a longer polymerisation time. The  $\text{Zr}(\text{IV})$  salalen complex was also assessed for activity in the ROP of *rac*-LA. For  $\text{Zr}(4)(\text{O}^t\text{Bu})_2$ , improved activity is observed relative to the  $\text{Ti}(\text{IV})$  salalen.

However, there is a large difference between observed and theoretical molecular weight values for the solution polymerisation, with a relatively broad distribution of chain lengths ( $\bar{D} = 1.34$ ). Both of these facts may indicate a slow initiation process, due to the disfavoured insertion of  $t\text{BuO}^-$  into the monomer.<sup>42</sup> To test this, polymerisation was carried out in the presence of one equivalence of  $\text{BnOH}$ . Under these conditions, the both molecular weight and distribution are reduced ( $\bar{D} = 1.21$ ) indicating an increase in control, which is mirrored by better agreement between theoretical and actual  $M_n$ . Furthermore, the polymerisation is observed to be more rapid (71%, 3 h). The solvent-free polymerisation achieves reasonable conversion within 30 minutes, however, a broad molecular weight distribution is observed under these conditions ( $\bar{D} = 1.42$ ). Under solution or melt conditions no stereocontrol is achieved by  $\text{Zr}(4)(\text{O}^t\text{Bu})_2$  (Table 4).

Unusually, attempts to polymerise *rac*-LA with the related  $\text{Zr}(\text{IV})$  salan,  $\text{Zr}(5)(\text{O}^t\text{Bu})_2$ , were unsuccessful in solution and for solvent-free reactions. For the five coordinate  $\text{Zr}(6)(\text{O}^t\text{Bu})_2$  complex, similar molecular weight control and activity is demonstrated in both solution and under melt conditions. However, closer examination of the homonuclear decoupled  $^1\text{H}$  spectrum for PLA derived from  $\text{Zr}(6)(\text{O}^t\text{Bu})_2$  shows an unusual enhancement of the *isi* resonance (see ESI†). This is due to stereorandom transesterification giving rise to polymer linkages not typically observed for *rac*-LA.<sup>60,78,79</sup> These linkages are determined to be related to *iss*, *sss*, and *ssi* tetrads from analysis of the methine region in the  $^{13}\text{C}\{^1\text{H}\}$  NMR spectrum (see ESI†) and should not be present for the ROP of *rac*-LA.<sup>80</sup>

**Table 4**  $\text{Zr}(\text{IV})$  complexes for polymerisation of *rac*-LA

Complex	Time/h	Conv. <sup>d</sup> , %	$P_t$ <sup>e</sup>	$M_{n,\text{theo}}^f$	$M_n^g$	$\bar{D}^g$
$\text{Zr}(1)_2(\text{O}^i\text{Pr})_2$ <sup>a</sup>	2	62	0.53	4500	2950	1.12
$\text{Zr}(1)_2(\text{O}^i\text{Pr})_2$ <sup>b</sup>	0.8	80	0.60	17 350	6950	1.17
$\text{Zr}(3)_2(\text{O}^i\text{Pr})_2$ <sup>a</sup>	6	63	0.45	4500	4000	1.07
$\text{Zr}(4)(\text{O}^t\text{Bu})_2$ <sup>a</sup>	4	72	0.53	5250	16 350	1.34
$\text{Zr}(4)(\text{O}^t\text{Bu})_2$ <sup>c</sup>	3	71	0.56	5200	5900	1.21
$\text{Zr}(4)(\text{O}^t\text{Bu})_2$ <sup>b</sup>	0.4	69	0.52	15 000	13 400	1.42
$\text{Zr}(6)(\text{O}^t\text{Bu})_2$ <sup>a</sup>	4	77	0.60	5600	6500	1.10
$\text{Zr}(6)(\text{O}^t\text{Bu})_2$ <sup>b</sup>	0.25	75	0.60	16 300	15 600	1.19

Conditions: <sup>a</sup>  $[\text{LA}]:[\text{I}] = 100:1$ , 80 °C, toluene. <sup>b</sup>  $[\text{LA}]:[\text{I}] = 300:1$ , 130 °C, solvent free. <sup>c</sup>  $[\text{LA}]:[\text{I}]:[\text{BnOH}] = 100:1:1$ , 80 °C, toluene. <sup>d</sup> Determined via  $^1\text{H}$  NMR spectroscopy. <sup>e</sup>  $P_t$  is the probability of hetero-tactic enchainment, determined via homonuclear decoupled  $^1\text{H}$  NMR spectroscopy. <sup>f</sup> Theoretical molecular weight calculated from conversion  $\{[\text{LA}]/[\text{I}] \times (\text{conv.} \times 144.13)/2 + M_n(\text{end group})\}$  (rounded to the nearest 50). <sup>g</sup> Determined from GPC (in THF) referenced against polystyrene standards with a correction factor of 0.58 applied.

These tetrads coincide with the *isi* resonance in the  $^1\text{H}$  NMR spectrum, hence the overall dominance of this resonance.

MALDI-ToF mass spectrometry analysis was performed on polymer derived from  $\text{Zr}(\text{IV})$  alkoxides (see ESI†). For  $\text{Zr}(1)_2(\text{O}^i\text{Pr})_2$ , in solution, the observed molecular weight series is higher than GPC and more consistent with the theoretical value ( $M_{n,\text{MALDI}} = 4200 \text{ g mol}^{-1}$ ). There is one major series with  $72 \text{ g mol}^{-1}$  spacing indicating transesterification reactions are occurring under these conditions, with  $i\text{PrO}^-$  and  $\text{H}^-$  end-groups. There is also evidence of cyclic PLA oligomers from application the of  $\text{Zr}(1)_2(\text{O}^i\text{Pr})_2$  as well as TFA (trifluoroacetic acid) capped polymer (the TFA is the counterion for the  $\text{Na}(\text{I})$  source in MALDI).

In another instance, a series related to methoxy capped PLA was observable due to washing with  $\text{MeOH}$ . The polymer derived from the solvent-free polymerisation was also amenable to MALDI-ToF analysis. Similar observations are made as for the solution polymerisation, with  $i\text{PrO}^-$ ,  $\text{H}^-$  and TFA- end-groups present as well as cyclic structures. For the solvent-free MALDI-ToF spectrum, the distribution is not symmetrical with a substantial tail to low molecular weight.  $\text{Zr}(3)_2(\text{O}^i\text{Pr})_2$  affords one main polymeric series with a spacing of  $72 \text{ g mol}^{-1}$  indicating the presence of undesirable transesterification reactions, however, the correct end groups are evident. For the salalen complex,  $\text{Zr}(5)(\text{O}^t\text{Bu})_2$ , the polymer prepared in the absence of co-initiator is too large to be analysed by MALDI-ToF. However, the addition of  $\text{BnOH}$  afforded lower molecular weights amenable to characterisation. The spectrum is dominated by polymer containing the expected  $\text{BnO}^-$  end group, with a symmetrical distribution and a  $72 \text{ g mol}^{-1}$  peak spacing. Trace amounts of  $t\text{BuO}^-$  capped polymer is observed at lower molecular weight. For polymer derived from  $\text{Zr}(6)(\text{O}^t\text{Bu})_2$ , there are no peaks associated with the expected  $t\text{BuO}^-$  end group via MALDI-ToF analysis. Instead, the main series, which has a spacing of  $72 \text{ g mol}^{-1}$ , correlates well with methoxy end groups. Evidently, transesterification or cyclic oligomer ring opening occurs during polymer work-up. A minor series is also present which is shown to possess no end-groups.





## Conclusions

Racemic ligands based upon 2-(aminomethyl)piperidine have been prepared and complexed to a range of metals. The majority of complexes reported are found to be diastereomeric in solution and characterised by a combination of X-ray crystallography and NMR spectroscopic methods. These complexes were assessed for their ability to polymerise lactide. For the Mg(II) and Zn(II) complexes, good activity and molecular weight control is generally achievable in solution. For Zn(1–2)<sub>2</sub>, immortal polymerisation was shown to be feasible. These complexes demonstrated activity under solvent free conditions. The Ti(IV) complexes were found to be relatively poor for the ROP of *rac*-LA with only Ti(5)(O<sup>i</sup>Pr)<sub>2</sub> demonstrating a controlled polymerisation. Increased activity and control was achievable with the Zr(IV) complexes, which is in agreement with literature precedent.

## Acknowledgements

We wish to thank the EPSRC for funding the CDT at Bath (EP/G03768X/1) and Purac for the donation of lactide. X-ray diffraction, NMR, MALDI-ToF and GPC facilities were provided through the Chemical Characterisation and Analysis Facility (CCAF) at the University of Bath.

## References

- M. R. Thomsett, T. E. Storr, O. R. Monaghan, R. A. Stockman and S. M. Howdle, *Green Mater.*, 2016, **4**, 115.
- R. Auras, B. Harte and S. Selke, *Macromol. Biosci.*, 2004, **4**, 835.
- R. Auras, S. Singh and J. Singh, *J. Test. Eval.*, 2006, **34**, 1.
- R. A. Auras, S. P. Singh and J. J. Singh, *Packag. Technol. Sci.*, 2005, **18**, 207.
- R. G. Sinclair, *J. Macromol. Sci., Pure Appl. Chem.*, 1996, **A33**, 585.
- E. T. H. Vink, D. A. Glassner, J. J. Kolstad, R. J. Wooley and R. P. O'Connor, *Ind. Biotechnol.*, 2007, **3**, 58.
- M. R. Yates and C. Y. Barlow, *Resour., Conserv. Recycl.*, 2013, **78**, 54.
- H. Tsuji, *Macromol. Biosci.*, 2005, **5**, 569.
- H.-L. Chen, S. Dutta, P.-Y. Huang and C.-C. Lin, *Organometallics*, 2012, **31**, 2016.
- E. D. Cross, L. E. N. Allan, A. Decken and M. P. Shaver, *J. Polym. Sci., Part A: Polym. Chem.*, 2013, **51**, 1137.
- P. Hormnirun, E. L. Marshall, V. C. Gibson, R. I. Pugh and A. J. P. White, *Proc. Natl. Acad. Sci. U. S. A.*, 2006, **103**, 15343.
- P. Hormnirun, E. L. Marshall, V. C. Gibson, A. J. P. White and D. J. Williams, *J. Am. Chem. Soc.*, 2004, **126**, 2688.
- S. M. Kirk, H. C. Quilter, A. Buchard, L. H. Thomas, G. Kociok-Kohn and M. D. Jones, *Dalton Trans.*, 2016, **45**, 13846.
- K. Majerska and A. Duda, *J. Am. Chem. Soc.*, 2004, **126**, 1026.
- P. McKeown, M. G. Davidson, G. Kociok-Kohn and M. D. Jones, *Chem. Commun.*, 2016, **52**, 10431.
- N. Nomura, R. Ishii, Y. Yamamoto and T. Kondo, *Chem. – Eur. J.*, 2007, **13**, 4433.
- A. Pilone, K. Press, I. Goldberg, M. Kol, M. Mazzeo and M. Lamberti, *J. Am. Chem. Soc.*, 2014, **136**, 2940.
- N. Spassky, M. Wisniewski, C. Pluta and A. LeBorgne, *Macromol. Chem. Phys.*, 1996, **197**, 2627.
- Z. Zhong, P. J. Dijkstra and J. Feijen, *J. Am. Chem. Soc.*, 2003, **125**, 11291.
- Z. Y. Zhong, P. J. Dijkstra and J. Feijen, *Angew. Chem., Int. Ed.*, 2002, **41**, 4510.
- M. D. Jones, L. Brady, P. McKeown, A. Buchard, P. M. Schafer, L. H. Thomas, M. F. Mahon, T. J. Woodman and J. P. Lowe, *Chem. Sci.*, 2015, **6**, 5034.
- P. McKeown, M. G. Davidson, J. P. Lowe, M. F. Mahon, L. H. Thomas, T. J. Woodman and M. D. Jones, *Dalton Trans.*, 2016, **45**, 5374.
- D. C. Aluthge, J. M. Ahn and P. Mehrkhodavandi, *Chem. Sci.*, 2015, **6**, 5284.
- D. C. Aluthge, B. O. Patrick and P. Mehrkhodavandi, *Chem. Commun.*, 2013, **49**, 4295.
- D. C. Aluthge, E. X. Yan, J. M. Ahn and P. Mehrkhodavandi, *Inorg. Chem.*, 2014, **53**, 6628.
- J.-C. Buffet, J. Okuda and P. L. Arnold, *Inorg. Chem.*, 2010, **49**, 419.
- M. Cybularczyk, M. Dranka, J. Zachara and P. Horeglad, *Organometallics*, 2016, **35**, 3311.
- A. F. Douglas, B. O. Patrick and P. Mehrkhodavandi, *Angew. Chem., Int. Ed.*, 2008, **120**, 2322.
- S. Ghosh, R. R. Gowda, R. Jagan and D. Chakraborty, *Dalton Trans.*, 2015, **44**, 10410.
- K. M. Osten, D. C. Aluthge and P. Mehrkhodavandi, *Dalton Trans.*, 2015, **44**, 6126.
- A. Pietrangelo, M. A. Hillmyer and W. B. Tolman, *Chem. Commun.*, 2009, 2736.
- I. Yu, A. Acosta-Ramírez and P. Mehrkhodavandi, *J. Am. Chem. Soc.*, 2012, **134**, 12758.
- Z. Dai, Y. Sun, J. Xiong, X. Pan, N. Tang and J. Wu, *Catal. Sci. Technol.*, 2016, **6**, 515.
- Z. Dai, Y. Sun, J. Xiong, X. Pan and J. Wu, *ACS Macro Lett.*, 2015, 556.
- Y. Sun, J. Xiong, Z. Dai, X. Pan, N. Tang and J. Wu, *Inorg. Chem.*, 2016, **55**, 136.
- J. Xiong, J. Zhang, Y. Sun, Z. Dai, X. Pan and J. Wu, *Inorg. Chem.*, 2015, **54**, 1737.
- J. Zhang, C. Jian, Y. Gao, L. Wang, N. Tang and J. Wu, *Inorg. Chem.*, 2012, **51**, 13380.
- J. Zhang, J. Xiong, Y. Sun, N. Tang and J. Wu, *Macromolecules*, 2014, **47**, 7789.
- A. Amgoune, C. M. Thomas, T. Roisnel and J.-F. Carpentier, *Chem. – Eur. J.*, 2006, **12**, 169.



- 40 P. L. Arnold, J.-C. Buffet, R. P. Blaudeck, S. Sujecki, A. J. Blake and C. Wilson, *Angew. Chem., Int. Ed.*, 2008, **47**, 6033.
- 41 C. Bakewell, T.-P.-A. Cao, X. F. Le Goff, N. J. Long, A. Auffrant and C. K. Williams, *Organometallics*, 2013, **32**, 1475.
- 42 C. Bakewell, T.-P.-A. Cao, N. Long, X. F. Le Goff, A. Auffrant and C. K. Williams, *J. Am. Chem. Soc.*, 2012, **134**, 20577.
- 43 C. Bakewell, A. J. P. White, N. J. Long and C. K. Williams, *Angew. Chem., Int. Ed.*, 2014, **53**, 9226.
- 44 C. Bakewell, A. J. P. White, N. J. Long and C. K. Williams, *Inorg. Chem.*, 2015, **54**, 2204.
- 45 T.-P.-A. Cao, A. Buchard, X. F. Le Goff, A. Auffrant and C. K. Williams, *Inorg. Chem.*, 2012, **51**, 2157.
- 46 Z. Mou, B. Liu, X. Liu, H. Xie, W. Rong, L. Li, S. Li and D. Cui, *Macromolecules*, 2014, **47**, 2233.
- 47 K. Nie, L. Fang, Y. Yao, Y. Zhang, Q. Shen and Y. Wang, *Inorg. Chem.*, 2012, **51**, 11133.
- 48 S. Yang, K. Nie, Y. Zhang, M. Xue, Y. Yao and Q. Shen, *Inorg. Chem.*, 2014, **53**, 105.
- 49 B. M. Chamberlain, M. Cheng, D. R. Moore, T. M. Ovitt, E. B. Lobkovsky and G. W. Coates, *J. Am. Chem. Soc.*, 2001, **123**, 3229.
- 50 M. H. Chisholm, J. Gallucci and K. Phomphrai, *Inorg. Chem.*, 2002, **41**, 2785.
- 51 H. Wang, J. Guo, Y. Yang and H. Ma, *Dalton Trans.*, 2016, **45**, 10942.
- 52 H. Wang and H. Ma, *Chem. Commun.*, 2013, **49**, 8686.
- 53 H. Wang, Y. Yang and H. Ma, *Macromolecules*, 2014, **47**, 7750.
- 54 H. Wang, Y. Yang and H. Ma, *Inorg. Chem.*, 2016, **55**, 7356.
- 55 S. Abbina and G. Du, *ACS Macro Lett.*, 2014, **3**, 689.
- 56 M. J. Walton, S. J. Lancaster and C. Redshaw, *ChemCatChem*, 2014, **6**, 1892.
- 57 H. Xie, Z. Mou, B. Liu, P. Li, W. Rong, S. Li and D. Cui, *Organometallics*, 2014, **33**, 722.
- 58 A. J. Chmura, D. M. Cousins, M. G. Davidson, M. D. Jones, M. D. Lunn and M. F. Mahon, *Dalton Trans.*, 2008, 1437.
- 59 E. L. Whitelaw, G. Loraine, M. F. Mahon and M. D. Jones, *Dalton Trans.*, 2011, **40**, 11469.
- 60 A. J. Chmura, M. G. Davidson, M. D. Jones, M. D. Lunn, M. F. Mahon, A. F. Johnson, P. Khunkamchoo, S. L. Roberts and S. S. F. Wong, *Macromolecules*, 2006, **39**, 7250.
- 61 M. D. Jones, S. L. Hancock, P. McKeown, P. M. Schafer, A. Buchard, L. H. Thomas, M. F. Mahon and J. P. Lowe, *Chem. Commun.*, 2014, **50**, 15967.
- 62 P. A. Cameron, V. C. Gibson, C. Redshaw, J. A. Segal, A. J. P. White and D. J. Williams, *J. Chem. Soc., Dalton Trans.*, 2002, 415.
- 63 L. Cuesta-Aluja, A. Campos-Carrasco, J. Castilla, M. Reguero, A. M. Masdeu-Bultó and A. Aghmiz, *J. CO<sub>2</sub> Util.*, 2016, **14**, 10.
- 64 J. B. L. Gallaway, J. R. K. McRae, A. Decken and M. P. Shaver, *Can. J. Chem.*, 2012, **90**, 419.
- 65 K. Press, A. Cohen, I. Goldberg, V. Venditto, M. Mazzeo and M. Kol, *Angew. Chem., Int. Ed.*, 2011, **50**, 3529.
- 66 E. L. Whitelaw, M. D. Jones and M. F. Mahon, *Inorg. Chem.*, 2010, **49**, 7176.
- 67 A. Yeori, S. Gendler, S. Groysman, I. Goldberg and M. Kol, *Inorg. Chem. Commun.*, 2004, **7**, 280.
- 68 E. Sergeeva, J. Kopilov, I. Goldberg and M. Kol, *Chem. Commun.*, 2009, 3053.
- 69 H. Glasner and E. Y. Tshuva, *Inorg. Chem.*, 2014, **53**, 3170.
- 70 J. Balsells, P. J. Carroll and P. J. Walsh, *Inorg. Chem.*, 2001, **40**, 5568.
- 71 A. Yeori, S. Groysman, I. Goldberg and M. Kol, *Inorg. Chem.*, 2005, **44**, 4466.
- 72 C. Fliedel, D. Vila-Viçosa, M. J. Calhorda, S. Dagorne and T. Avilés, *ChemCatChem*, 2014, **6**, 1357.
- 73 E. L. Whitelaw, M. G. Davidson and M. D. Jones, *Chem. Commun.*, 2011, **47**, 10004.
- 74 A. J. Chmura, M. G. Davidson, M. D. Jones, M. D. Lunn and M. F. Mahon, *Dalton Trans.*, 2006, 887.
- 75 S. Gendler, S. Segal, I. Goldberg, Z. Goldschmidt and M. Kol, *Inorg. Chem.*, 2006, **45**, 4783.
- 76 M. Kol, M. Shamis, I. Goldberg, Z. Goldschmidt, S. Alfi and E. Hayut-Salant, *Inorg. Chem. Commun.*, 2001, **4**, 177.
- 77 A. L. Zelikoff, J. Kopilov, I. Goldberg, G. W. Coates and M. Kol, *Chem. Commun.*, 2009, 6804.
- 78 M. Bero, J. Kasperczyk and Z. J. Jedlinski, *Makromol. Chem.*, 1990, **191**, 2287.
- 79 B. Calvo, M. G. Davidson and D. García-Vivó, *Inorg. Chem.*, 2011, **50**, 3589.
- 80 M. T. Zell, B. E. Padden, A. J. Paterick, K. A. M. Thakur, R. T. Kean, M. A. Hillmyer and E. J. Munson, *Macromolecules*, 2002, **35**, 7700.

